Generic two-variable model of excitability

A. C. Ventura, G. B. Mindlin, and S. Ponce Dawson
Departamento de Física, FCEN, UBA Ciudad Universitaria, Pabellón I (1428), Buenos Aires, Argentina
(Received 18 October 2001; published 10 April 2002)

We present a simple model that displays all classes of two-dimensional excitable regimes. One of the variables of the model displays the usual spikes observed in excitable systems. Since the model is written in terms of a ''standard'' vector field, it is always possible to fit it to experimental data displaying spikes in an algorithmic way. In fact, we use it to fit a series of membrane potential recordings obtained in the medicinal leech and time series generated with the FitzHugh-Nagumo equations and the excitability model of Eguía *et al.* [Phys. Rev. E **58**, 2636 (1998)]. In each case, we determine the excitability class of the corresponding system.

DOI: 10.1103/PhysRevE.65.046231 PACS number(s): 05.40.Ca, 05.45.−a, 42.55.Px

I. INTRODUCTION

Excitable systems are ubiquitous in nature [1]. Excitability is mainly a concept of biological origin and there is no sharp mathematical definition of its meaning. It involves the existence of a stable stationary solution (a fixed point) and a threshold. Perturbations to this fixed point that are below this threshold make the system go back to the fixed point with an almost linear dynamics. Perturbations above this threshold, on the other hand, make the system undergo long excursions in phase space before going back to the fixed point. Usually, for the dynamics to be excitable it is also required that this long excursion be independent of the initial condition (after a very short transient). The paradigmatic example of excitable dynamics is that of neuronal action potentials [2]. Yet, other examples exist in as diverse systems as semiconductor lasers with optical feedback [3], reaction-diffusion systems [4], etc.

The minimum dimensionality of an Euclidean phase space in which a dynamical system can display excitability is two. Yet, even in such a simple case, different scenarios have been proposed, compatible with the definition of excitability described before. For example, in neuroscience it is customary to refer to excitability of class I and II [2]. In class I excitability, the excitable nature of the dynamics is lost at a Hopf bifurcation, where a periodic orbit of finite frequency and zero amplitude is born. The fixed point (stationary state in the excitable regime) loses its stability but continues to exist. Class II comprises the systems in which the excitable nature is lost at an Andronov bifurcation, i.e., where a periodic orbit of infinite period and finite amplitude is born. In this case, the stationary state of the excitable regime dissapears at an inverse saddle-node bifurcation. This classification was first suggested by Hodgkin in 1948 [2].

Several dynamical models are used to describe excitable behavior. One of the most commonly used ones is the FitzHugh-Nagumo model [4], particularly for parameter values in which excitability of class I is present. The model is given by

$$v' = v - \frac{v^3}{3} - w + i,$$

$$w' = \Phi(v + a - bw), \qquad (1)$$

where the primes stand for time derivatives. It corresponds to a two-dimensional caricature of the phenomenological Hodgkin-Huxley system of equations that describe the behavior of the membrane potential and ion conductances in the squid giant axon [5]. One of the two variables in the FitzHugh-Nagumo model (v) plays the role of the membrane potential, while the second variable (w) plays the role of all three other variables accounting for the conductances in the original Hodgkin-Huxley model. Dynamically, this simplified model behaves as displayed in Fig. 1(a). For low values of the parameter i, which represents an external current that is applied to the neuron, the system is excitable. Beyond a critical value of the parameter, an oscillatory motion takes place. The bifurcation behind this qualitative change is a Hopf bifurcation [2].

Other researchers use Adler's equation as a paradigm of excitability. This equation describes the dynamics of an angular phase θ displaying excitability of class II. The behavior of the system, ruled by $d\theta/dt = \mu - \cos(\theta)$ is qualitatively different for μ larger or smaller than one. In the first case,

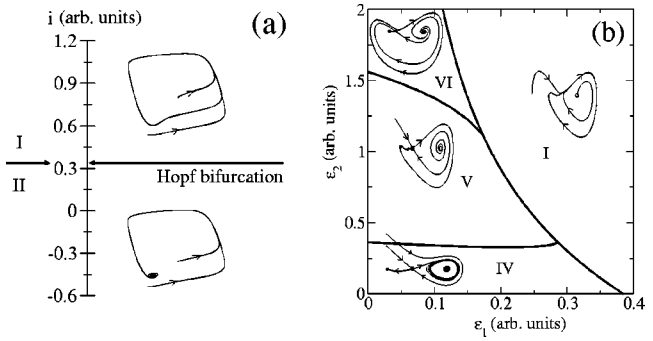

FIG. 1. Examples of class I (a) and class II (b) excitability. (a) The Fitzhugh-Nagumo model, given by Eqs. (1) with $\Phi = 0.08$, $a = 0.7$, and $b = 0.8$. (b) The model of Ref. [6], given by Eqs. (2). In both figures, each region corresponds to a particular topological behavior. Different regions are separated by bifurcation curves or points. We have used the same set of labels throughout the paper. In particular, label I corresponds to a situation with one stable limit cycle and a repellor, label II to a situation with one stable fixed point and label V to a situation with one stable fixed point, a saddle, and a repellor. The curve separating region V from region I in (b) corresponds to an Andronov bifurcation, and the point in (a) separating region I and II corresponds to a Hopf bifurcation.

the variable θ increases monotonically. In the latter case, the system presents two fixed points, one of them attracting. If the system is perturbed from this state beyond the unstable fixed point, the decay onto the stationary solution occurs after a large excursion in phase space. Other systems continue to be presented in the literature. A two-dimensional model for Euclidean variables was recently introduced to account for class II excitability [6]. In this model, which is given by the following equations:

$$x' = y,$$

$$y' = x - y - x^3 + xy + \epsilon_1 + \epsilon_2 x^2, \tag{2}$$

excitability occurs as shown in region V of Fig. 1(b). Three fixed points are present in this region: an attractor, a saddle, and a repellor. If the system is perturbed away from the attractor beyond the saddle point's stable manifold, a large excursion in phase space takes place. As in Adler's system, the loss of excitability towards the oscillatory regime occurs as the saddle and the attractor collide at a saddle-node bifurcation. The global connection of the manifolds guarantees the appearance of oscillations, which are born with nonzero amplitude. These oscillations are born at the curve separating regions V and I in Fig. 1(b).

Excitable systems of class I and II present different collective behavior when coupled [2]. Coupling effectively leads the individual (coupled) units to cross the corresponding bifurcation, generating oscillations. In the case of class I units the frequency of the resulting oscillations is clustered around a well-defined mean value, determined by the Hopf bifurcation. In the case of class II excitable units, the situation is different: at an Andronov bifurcation, oscillations are born with zero frequency. This frequency typically changes very fast with the parameter as its value is moved away from the bifurcation value. Therefore, when coupling class II excitable units there is a large range of available frequencies, which gives rise to collective behaviors that can be distinguished from those observed in populations of coupled class I systems. Noise also produces different signatures on each class, because of the same reason. Therefore, it is of interest to distinguish between both types. In spite of this, achieving a unified description is always appealing among other reasons, because of the simplicity of having a single model, instead of many different ones. A single model would provide an understanding of the basic common features underlying all classes of excitability. In the case of coupled units, having a unified description would allow one to study transitions among behaviors that so far have been studied within a restricted model and, in doing so, it would be possible to find different, unexplored behaviors. Needless to say, understanding the way in which a property of an excitable unit translates into a particular collective behavior is a most important issue since, in living organisms, excitable cells are interconnected forming populations that can display emergent behavior.

The reason for the variety of models of excitability that are present in the literature lies in the global nature of the dynamical components that are necessary to build an excitable model. This contrasts with what occurs near local bifurcations. Namely, for nonlinear systems with a singular fixed point there is an algorithmic prescription to reduce the number of terms in the equations that rule the dynamics in a neighborhood of the singular fixed point (a procedure known as normal form construction, see, e.g., [7]). However, unfolding theory provides some tools to obtain global information from local analyses [8]. Building upon these ideas, we provide in this paper a generic model that is able to display all two dimensional scenarios of excitability. Furthermore, the model generates spiking signals, typical of excitable dynamics. Since its defining dynamical equations are written in a standard form, experimental data with spikes can be fitted by our model in a simple and algorithmic way. In principle, this would mean that a single set of equations could be used to decide whether an experimentally observed excitable system with spikes was of class I or class II. Although we successfully identified the right excitability class when fitting data that had been generated with systems of known class, we cannot guarantee that this suggestive result will apply to an arbitrary system. In general, the identification of the excitability class requires either being able to explore the bifurcation in the deterministic case or inspecting the behavior of the system under the influence of noise.

The organization of the paper is as follows. In Sec. II we present the model. In Sec. III we use it to fit neuronal recordings from the medicinal leech and other time series obtained from well known models of excitable dynamics. In Sec. IV we analyze its role in reaction-diffusion systems. Finally the conclusions are summarized in Sec. V.

II. BUILDING A GENERIC MODEL OF EXCITABILITY

The fact that excitability is a feature that relies on global properties precludes, in principle, a systematic model derivation. This is the reason underlying the large variety of models that appear in the literature. However, as stated in Ref. [8], given a system with a (very) degenerate singularity, the local study of the degenerate diagram and of its perturbations contains information that is of global character for the (less degenerate) perturbations of the singular vector field. This statement provides a clue of how to go around the problem of the global features of excitability. Namely, we will look for a singular vector field with a degenerate bifurcation diagram that can unfold into less degenerate ones, some of which display class I and some of which display class II excitability. The first necessary feature of the model is the existence of a (stable) fixed point. On the other hand, we need a singular vector field such that, arbitrarily close to it (in the space of vector fields) there are (i) vector fields with a stable limit cycle whose size goes to zero as we get closer to the singular vector field, (ii) vector fields with three fixed points, a pair of which is able to collide at a saddle-node bifurcation. The winged cusp is the example of a degenerate system in which a single fixed point can split up in three. Furthermore, the unfolding of the cusp contains diagrams where these fixed points can collide (in pairs) at saddle-node bifurcations. Therefore, we want to combine the cusp with a Hopf bifurcation. In a way, we are looking at the (degener-

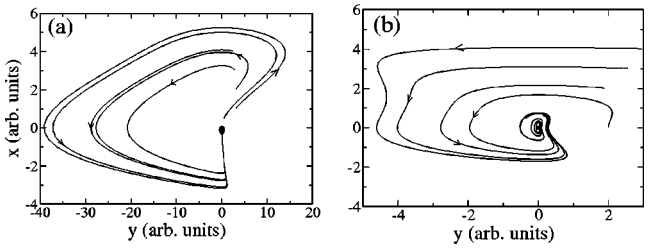

FIG. 2. Behavior of the system Eqs. (4) for $\epsilon=0.2$ (a) and $\epsilon=1$ (b) and various initial conditions. Notice the different scale on the horizontal axis, which reflects the fact that phase space excursions become very large as ϵ decreases.

ate) two-dimensional system with only one fixed point that results from the collapse of one limit cycle and three fixed points [9]. The linear part of the resulting degenerate vector field, at the fixed point, is the nilpotent matrix $\left(\begin{smallmatrix}0&1\\0&0\end{smallmatrix}\right)$. Any vector field with such a linear part can be written, up to third order, as [10]

$$x'=y,$$

$$y'=Ax^2+Bxy+Cx^2y+Dx^3. \tag{3}$$

This corresponds to the Takens-Bogdanov normal form up to third order. We keep terms of up to third in order to guarantee the existence of up to three fixed points in the unfolding of the degenerate system we are seeking. Now, for general values, A and D, Eqs. (3) have two fixed points: (0,0) and $(-A/D,0)$. Therefore, we set $A=0$ in order to have a unique fixed point. Rescaling the variables, x, y, and time, Eqs. (3) can be rewritten as

$$x'=y,$$

$$y'=\frac{1}{\epsilon}xy-x^2y-x^3, \tag{4}$$

where $\epsilon>0$ and the choice of negative cubic coefficients guarantees the global attractive nature of the unique fixed point, $x=0$, $y=0$. Equation (4) is the degenerate system whose unfolding provides the expected generic model of excitability. It corresponds to a third-order Takens-Bogdanov normal form in which some of the quadratic coefficients vanish. The parameter ϵ provides a measure of how excitable the system is. As illustrated in Fig. 2 the smaller the ϵ the more excitable the system is, as reflected in both the size of the excursion in phase space after the fixed point is perturbed and how fast the trajectory eventually becomes independent of the initial condition.

We show now that an unfolding of this singular vector field, given by

$$x'=y,$$

$$y'=\mu_0+\mu_1x+\mu_2y+\frac{1}{\epsilon}xy-x^3-x^2y, \tag{5}$$

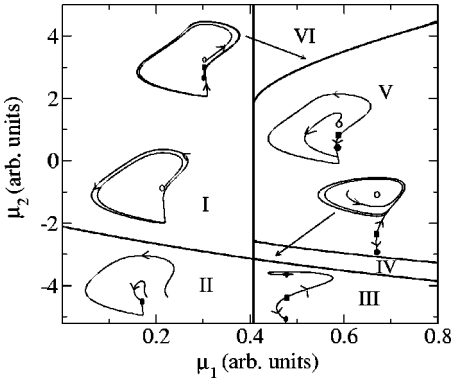

FIG. 3. The bifurcation diagram of the generic model of excitability given by Eqs. (5) with $\epsilon=0.2$ and $\mu_0=0.1$. Both the diagrams of class I and class II excitability (see Fig. 1) are contained in it.

is able to display the different two-dimensional scenarios of excitability described in the Introduction. In Fig. 3, we display the phase portraits of the system for $\mu_0=0.1$ and $\epsilon=0.2$. Notice that in region I we find the typical two-dimensional excitability scenario associated to the FitzHugh-Nagumo equations (class I excitabilty). As μ_2 is increased, a Hopf bifurcation takes place giving rise to oscillatory behavior (as observed in region II). Interesting enough, in this phase portrait, this oscillation is destroyed at an Andronov bifurcation as μ_1 is increased towards region V, where three fixed point coexist: an attracting fixed point, a saddle, and a repellor. In region V, the stable manifold of the saddle acts as a threshold for perturbations of the attractor, as it is typical of class II excitability. Notice that we have labeled each topologically distinct dynamical behavior with a different number, keeping the same labeling as that in Fig. 1.

We have not proved that the unfolding (5) of Eqs. (4) is universal [8]. However, it does contain all the behaviors that characterize the different models of excitability in the plane. This means that the model, as a family of flows that depends on a set of parameters, not only displays excitable behavior for certain parameter values but also undergoes the bifurcations that models of class I and class II excitability undergo. This means that, given an excitable system of either class I or class II, there is a change of variables that takes the corresponding model system of equations into the form (5), at least for a range of parameter values that include the excitable behavior and the bifurcation that characterizes the bifurcation class.

Depending on the parameter values, variable x displays the typical spikes observed in excitable systems (see Figs. 4–6). Thus, the model not only displays behaviors that are topologically equivalent to those observed in models of class I and class II excitability, but is also able to reproduce the ''shape'' of the corresponding spiking signals. Thus, given a spiking signal produced by an excitable system, we expect to find a set of parameters for which our model fits the signal. It is important to note that the vector field in Eqs. (5) is standard, i.e., the dynamical variables are related to each other by means of temporal derivation. Thus, the fitting of the model to the observed spiking signals is always possible and algo-

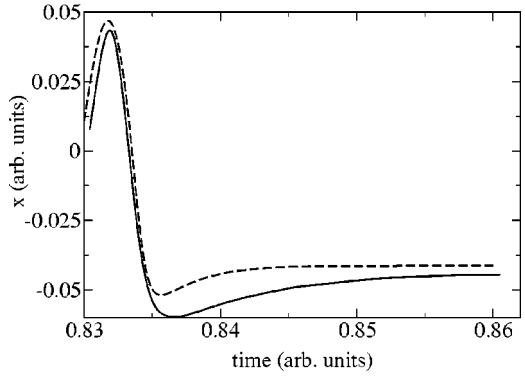

FIG. 4. Membrane potential as a funcion of time recorded in an experiment done with the medicinal leech (solid line) and best fit using the variable $x(t)$ of the generic model Eqs. (5) (dashed line).

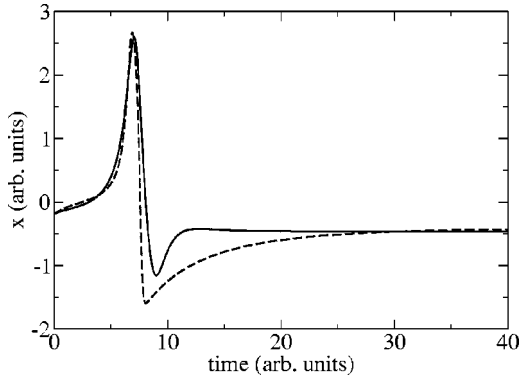

FIG. 6. Time series of y vs t obtained using Eqs. (2) with $\epsilon_1 = 0.15$ and $\epsilon_2 = 1$ (solid line) and best fit using the variable $x(t)$ of the generic model Eqs. (5) (dashed line).

rithmic [11]. We show several examples in the following section.

III. REPRODUCING OBSERVATIONS WITH THE MODEL

In this section we probe the ability of our model to reproduce the spiking signals observed in three different excitable systems. The first system we analyze corresponds to an experimental record of the membrane potential of a particular neuron in the medicinal leech [12]. The neuron propagates an action potential upon stimulation. We show in Fig. 4 one action potential that arises due to a stimulus in the form of a square pulse of finite duration (solid line) and the equivalent signal that we obtain using our model Eqs. (5) (dashed line). We fitted the experimental record once the stimulation was turned off: had we also included the part while the stimulus was on, we should have coupled our model equations to a time-dependent stimulus. Basically, we wrote down our generic model in the general form

$$x' = y,$$

$$y' = A + Bx + Cy + Dxy - Ex^3 - Fx^2y, \tag{6}$$

determined the values of A, B, C, D, E, and F that provided the best fit of $x(t)$ to the data and then rescaled the variables so as to go back to the form (5). In this way we could determine the region of parameter space where the fitting model belonged to. This is displayed in Fig. 7(a), where we have plotted a two-dimensional cut of the four-dimensional parameter space of Eqs. (5) that contained the point with the fitting parameter values (the asterisk in the figure). In particular, we can observe that the best fit corresponds to a region with only one fixed point. On the other hand, the fitting procedure provided a value of $\epsilon = 0.333$, which indicates the excitability of the system. Given another set of experimental data, a similar procedure could have been used to determine a higher dimensional model for the current system when coupled to the time-dependent stimulus. In particular, if we had a data set obtained with a square pulse stimulus of long enough duration, it would have been possible to fit the model in such a case and determine the parameters that are mostly affected due to the stimulus. In this way, it would have been possible to construct the higher dimensional model mentioned before.

We show in Fig. 5 the plot of a time series obtained via a numerical simulation of the FitzHugh-Nagumo equations (1) (solid line) and two series that we obtained using our model Eqs. (5) (dashed line). The simulation of the FitzHugh-Nagumo equations was done using $i = 0$, $\Phi = 0.08$, $a = 0.7$, and $b = 0.8$ for which Eqs. (1) have only one fixed point, which is stable. In this case we found one fit that reproduced very well the spiking part of the signal, but which tended quite slowly to the fixed point [shown in Fig. 5(b)] and another one that reproduced better the approach to the fixed

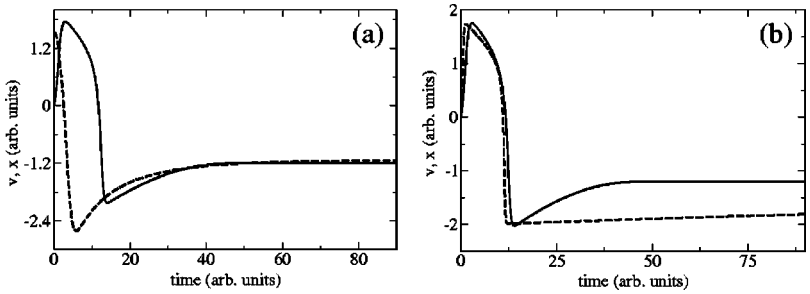

FIG. 5. Time series of v vs t obtained using the FitzHugh-Nagumo (1) with $i = 0$, $\Phi = 0.08$, $a = 0.7$, and $b = 0.8$ (solid line) and two possible fits using the variable $x(t)$ of the generic model Eqs. (5) (dashed line). The fit in (a) reproduces the approach towards the fixed point very accurately, while the one in (b) reproduces the spiking part of the signal better, but tends quite slowly to the fixed point. In any case, the flows generated with both sets of parameter values are topologically equivalent to one another.

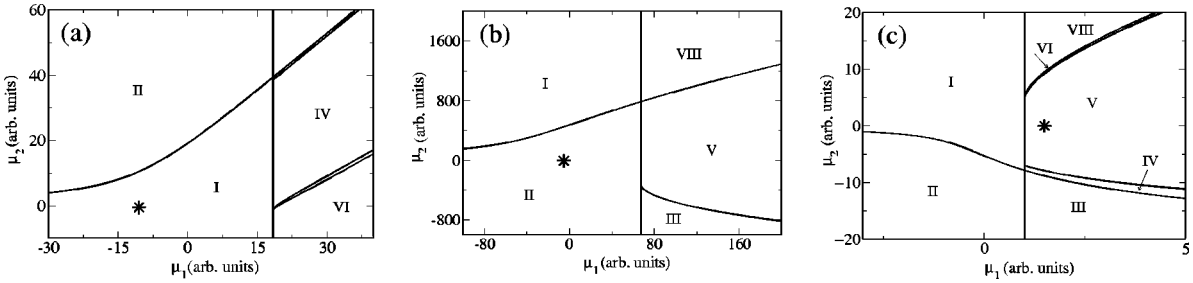

FIG. 7. Location in parameter space of the parameter values that give the best fits displayed in Fig. 4(a), Fig. 5(b), and Fig. 6(c). In (a) the values of the other two parameters are: $\epsilon=0.333$, $\mu_0=-30.5$, in (b) they are $\epsilon=0.0136$, $\mu_0=-213$, and in (c) $\epsilon=0.126$, $\mu_0=0.395$.

point [shown in Fig. 5(a)]. In either case, the parameter values of the generic model (5) belong to a similar region (a region with only one fixed point). We show the location of the set of parameter values that corresponds to the fit of Fig. 5(a) in Fig. 7(b). In this case, we obtained $\epsilon=0.0136$, an indication that the system is very excitable.

Finally, we fitted a data set obtained via a numerical simulation of Eqs. (2). We show the data (solid line) and the corresponding fit (dashed line) in Fig. 6. The simulation of Eqs. (2) was done using $\epsilon_1=0.15$ and $\epsilon_2=1$, for which the system lies in the region V of Fig. 1 (b). The fitting also provides a set of parameter values for which the model system (5) has one stable fixed point, one saddle, and one repellor. The value of ϵ obtained in this case is $\epsilon=0.13$.

In the case of the fits to numerically generated data (Figs. 5 and 6), a comparison of the location of the parameter values in Fig. 7 with those that were used to generate the data sets shows that the model is able to reproduce the right time evolution in a region of parameter values in which the model system is topologically equivalent to the systems that generated the data sets. Furthermore, in the case of system (2) we also fitted data sets generated with parameter values that were closer, in parameter space, to the Andronov bifurcation [the curve separating regions V and I in Fig. 1(b)] obtaining fitting parameter values that were also closer to the Andronov bifurcation in the model system (5). Finally, the values of ϵ obtained with the various fits provide some quantitative measure of the excitability of the system. As mentioned in the preceding section, small values of the parameter ϵ in the model system (5) correspond to large excursions in phase space before the system relaxes back to the fixed point and to fast decays onto a trajectory that is independent of the initial condition, two features of excitability. Thus, by fitting the model system to various data we also obtain some sort of quantitative comparison of their excitability. In this respect we could say that the data set in Fig. 5 is more excitable than the one in Fig. 6 and this one, in turn, is slightly more excitable than the one in Fig. 4.

IV. EXCITABLE REACTION-DIFFUSION SYSTEMS

So far we have focused on systems that can be described by sets of ordinary differential equations. However, excitability is also displayed by spatially extended systems and, sometimes, it is even defined within this setting. In particular, in one-space dimension, an excitable (extended) system can be defined as one that has a stable homogeneous stationary solution, which also supports a traveling pulse (see, e.g., [13]). This definition is also inspired in pulse propagation in nerves. Spatially extended excitable systems are usually of reaction-diffusion type. Reaction-diffusion systems describe the dynamics of dilute chemical components in solution. Their study has increased steadily during the last years for their possible applications to living organisms [4]. Reaction-diffusion systems display a large variety of patterns. It has recently been proposed that the ubiquity of some of the patterns and transitions observed in reaction-diffusion systems [14] can be attributed to the underlying spatially homogeneous dynamics when this dynamics is described by a planar vector field [15]. In particular, for the case of sets of two reaction-diffusion equations, it has been argued that the existence and properties of certain patterns can be understood in terms of the collection of planar vector fields that can be constructed via perturbations of the spatially homogeneous evolution equations [16]. This idea has been applied to the Gray-Scott model [17,18]

$$\frac{\partial u}{\partial t}=-uv^2+A(1-u)+D_u\nabla^2 u, \tag{7}$$

$$\frac{\partial v}{\partial t}=uv^2-Bv+D_v\nabla^2 v, \tag{8}$$

to explain why it could display patterns that were similar to those observed in the ferrocyanide-iodide-sulfite (FIS) reaction [14], although the Gray-Scott model did not correspond to an accurate representation of the chemical kinetics of the FIS reaction.

In the spatially homogeneous case the systems (7) and (8) has one fixed point, $u=1$, $v=0$, that is stable for all positive A and B (the physically relevant region, which we will analyze in this paper). This stable fixed point can either be the only one or can coexist with other two. For values of A and B for which the only spatially homogeneous fixed point is $u=1$, $v=0$, the spatially extended systems (7) and (8) display a large variety of patterns [18]. These patterns arise as a response to a finite perturbation. Namely, initial conditions that are arbitrarily close to the homogeneous fixed point relax back to it, and a larger (finite) perturbation is necessary for the system to settle onto a spatially inhomogeneous pat-

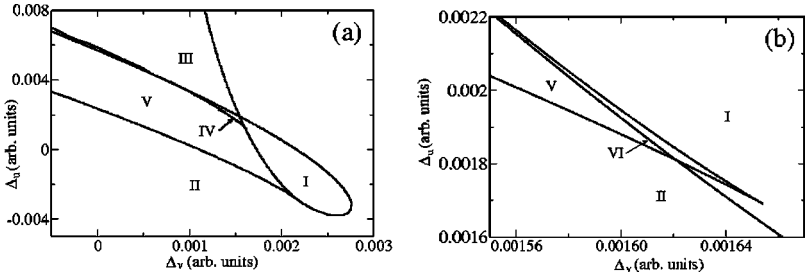

FIG. 8. The bifurcation set of the planar vector field (9) for $A=0.02$ and $B=0.08$ (a) and for $A=0.011$ and $B=0.08$ (b).

tern (that can also be time dependent). Thus, the spatially extended system is ''excitable.'' In particular, it is excitable for the parameter values at which spot replications are observed. In Ref. [16] we argued that this excitable behavior could be related to the proximity in parameter space to a saddle-repellor bifurcation, in such a way that diffusion effectively acted as a perturbation that let the system ''cross'' the bifurcation.

One way to analyze the possible behaviors that the system may visit due to the effect of diffusion is to study the system of Eqs. (7) and (8) as a planar vector field with the diffusion terms treated as parameters, $\Delta u \equiv D_u \nabla^2 u$, $\Delta v \equiv D_v \nabla^2 v$

$$u' = -uv^2 + A(1-u) + \Delta u,$$

$$v' = uv^2 - Bv + \Delta v. \tag{9}$$

Equations (9) may be reduced to Eqs. (5) for values of A and B nearby those at which spot replications may be observed. In particular, for $A=0.02$, $B=0.08$, the reaction-diffusion systems (7) and (8) display spot replications for $D_u=1$ and $D_v=0.5$. We have found that for these values of A and B, $\Delta u = \frac{8}{9}\sqrt{3AB} - A \approx -0.0026$ and $\Delta v = \sqrt{3AB}/9 \approx 0.0022$, Eqs. (9) have one fixed point at $u^* = 2\sqrt{3AB}/3A \approx 0.653$ and $v^* = \sqrt{A/3} \approx 0.082$ with two zero eigenvalues. Defining new variables that are zero at this fixed point, performing the linear changes required to transform the linear part of the vector field into its associated Jordan form, keeping nonlinear terms up to third order, and carrying the nonlinear changes of variables required to write the system in its normal form, we obtain that, at these parameter values, Eqs. (9) can be reduced to

$$x' = y,$$

$$y' = 1.73xy - x^3 - x^2 y, \tag{10}$$

in a neighborhood of the fixed point $u=0.653$ and $v=0.082$. Clearly, Eqs. (10) are equal to Eqs. (4) with $\epsilon = 0.58$. Hence, Eqs. (9) for parameter values in a neighborhood of the chosen ones should include both two-dimensional excitable regimes. This is, in fact, displayed in Fig. 8 where we have plotted the bifurcation set of Eqs. (9) on two two-dimensional cuts of its four-dimensional parameter space, in a neighborhood of the parameter values $A=0.02$, $B=0.08$, $\Delta u = -0.0026$, and $\Delta v = 0.0022$. Figure 8(a) corresponds to a cut with $A=0.02$, $B=0.08$ and Fig. 8(b) to one with $A=0.011$, $B=0.08$. Class I excitability is contained in Fig. 8(a), where region II corresponds to a situation with one excitable fixed point that undergoes a Hopf bifurcation on the curve that separates regions II and I. In particular, in region I there is one repellor surrounded by a stable limit cycle. Class II excitability is contained in both Figs. 8(a) and 8(b). In fact, all four topologically distinct behaviors displayed in Fig. 1(b) are contained in Fig. 8, although it is not easy to resolve all regions within the scale of the figures. In particular, region VI is too narrow but we have anyway indicated its approximate location with an arrow. In any case, the main feature of class II excitability, the Andronov bifurcation, appears in Fig. 8 (it occurs on the curve that separates regions V and I).

Figure 8 is an indication that the excitable features displayed by the Gray-Scott reaction-diffusion sytems (7) and (8) at $A=0.02$, $B=0.08$, could be related to the fact that diffusion effectively perturbs the system making it display the different classes of excitability encountered in other systems. Although we do not have a proof for this, having been able to find our generic model in a simple extension of the Gray-Scott system [Eqs. (9)] provides a useful set within which spatiotemporal excitability can be studied. As mentioned before, models of spatially extended excitable systems are usually of reaction-diffusion type. On the other hand, reaction-diffusion systems are usually analyzed in terms of inhibitor-activator systems. The Gray-Scott systems (7) and (8) is a reaction-diffusion system of inhibitor-activator type, with u the inhibitor and v the activator. If we add a constant parameter Δu to Eq. (7) and a constant parameter Δv to Eq. (8), the resulting system,

$$\frac{\partial u}{\partial t} = -uv^2 + A(1-u) + \Delta u + D_u \nabla^2 u$$

$$\frac{\partial v}{\partial t} = uv^2 - Bv + \Delta v + D_v \nabla^2 v, \tag{11}$$

still remains as an inhibitor-activator system. In the spatially homogeneous case, this extended system reduces to our general model of excitability (5) for certain parameter values. Therefore, this simple extension of the Gray-Scott model can be used to analyze the transition of spatiotemporal solutions of excitable reaction-diffusion systems of inhibitor-activator type when the underlying homogeneous dynamics changes from being of class I to being of class II excitability. We think that this can be a very useful tool to study excitable reaction-diffusion systems.

V. CONCLUSIONS

We have found a simple two-dimensional model [Eqs. (5)] that is able to display all dynamical behaviors encoun-

tered in models of class I and class II excitability. One of the variables of the model (x) displays the spiking signals that are typical of excitable systems. Given that the model equations are written in standard form, fitting the model to observed spiking signals is always possible and algorithmic. In fact, we have shown the ability of the model to reproduce both experimental and numerically generated data obtained with different sorts of excitable systems. In this way, for the cases analyzed, we could determine the excitability class to which the system that generated the signal belongs. Furthermore, we also obtained a quantitative assessment of their excitability by looking at the value of one of the fitting parameters (ϵ).

We have found that the Gray-Scott reaction-diffusion systems (7) and (8) contain the generic model [Eqs. (5)] when the diffusion terms are treated as parameters [as in Eqs. (9)]. Thus, we think that the sort of excitable behavior that the reaction-diffusion Gray-Scott system displays for certain parameter values can be understood as a consequence of the fact that diffusion perturbs the underlying homogeneous dynamics in such a way that it effectively visits the behaviors displayed by our generic model of excitability. On the other hand, we have shown that a simple extension of the Gray-Scott model [Eqs. (11)] provides an inhibitor-activator reaction-diffusion system that, in the spatially homogeneous limit, is able to display both class I and class II excitability. Thus, using Eqs. (11) it should be possible to study the relationship between different types of reaction-diffusion excitable systems by continuous prolongations of specific solutions.

In conclusion, we have presented a general and simple model that provides a unifying setting within which the various features of excitability can be studied.

[1] P.C. Coullet, S.C. Müller, and D. Walgraef, Chaos **4**, 439 (1994).

[2] F.C. Hoppensteadt and E.M. Izhikevich, *Weakly Connected Neural Networks* (Springer, New York, 1997).

[3] A.M. Yacomotti, M.C. Eguía, J. Aliaga, O.E. Martínez, G.B. Mindlin, and A. Lipsich, Phys. Rev. Lett. **83**, 292 (1999).

[4] J.D. Murray, *Mathematical Biology* (Springer, New York, 1989).

[5] A.L. Hodgkin and A.F. Huxley, J. Physiol. (London) **117**, 500 (1952).

[6] M.C. Eguía, G.B. Mindlin, and M. Giudici, Phys. Rev. E **58**, 2636 (1998).

[7] J. Guckenheimer and P. Holmes, *Nonlinear Oscillations, Dynamical Systems and Bifurcations of Vector Fields* (Springer, New York, 1986), p. 365.

[8] M. Golubitsky and D.G. Schaeffer, *Singularities and Groups in Bifurcation Theory* (Springer, New York, 1985), Vol. I, p. 121.

[9] The complete analysis of the codimension three cusp-Hopf bifurcation was recently carried out by J. Harlim and W.F. Langford, and involves a set of three ordinary differential equations [J. Harlim (private communication)].

[10] D.K. Arrowsmith and C.M. Place, *An Introduction to Dynamical Systems* (Cambridge University Press, Cambridge, 1990), p. 76.

[11] G. Gouesbet, Phys. Rev. A **43**, 5321 (1991).

[12] The data was provided by L. Szczupak (Department of Biology, FCEN, UBA). The membrane potential was recorded every 2 ms. Since the large excursion part of the action potentials last 10 ms, the data were interpolated with a cubic spline.

[13] T. Ohta, Y. Hayase, and R. Kobayashi, Phys. Rev. E **54**, 6074 (1996).

[14] K.J. Lee, W.D. McCormick, J.E. Pearson, and H.L. Swinney, Nature (London) **369**, 215 (1994).

[15] S. Ponce Dawson, M.V. D'Angelo, and J.E. Pearson, Phys. Lett. A **265**, 346 (2000)

[16] M.V. D'Angelo and S. Ponce Dawson (unpublished).

[17] P. Gray and S. Scott, Chem. Eng. Sci. **38**, 29 (1983).

[18] J.E. Pearson, Science **261**, 189 (1993).